

New J. Chem.

Supporting information available for

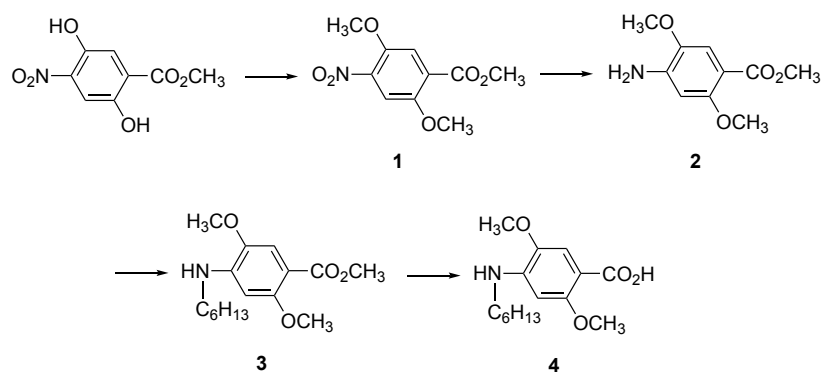
Stereoselectivity in Dehydrative Cyclic Trimerization of Substituted 4-Alkylaminobenzoic

Acids

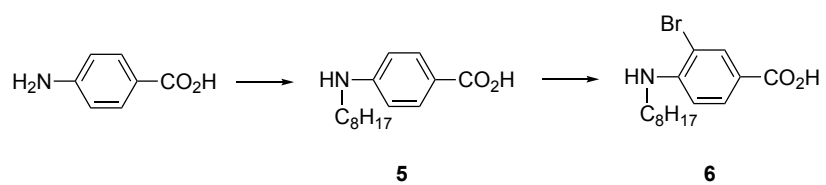
Koji Takagi,^{1*} Hinako Yamaguchi,¹ Daiki Miyamoto,¹ Yuka Deguchi,¹ Takehiro Hirao,² and
Takeharu Haino²

¹ Graduate School of Engineering, Nagoya Institute of Technology, Gokiso-cho, Showa-ku, Nagoya,
Aichi 466-8555

² Graduate School of Advanced Science and Engineering, Hiroshima University, 1-3-1
Kagamiyama, Higashi-Hiroshima, Hiroshima 739-8526



Scheme S1. Synthetic route to 2,5-dimethoxy monomer.



Scheme S2. Synthetic route to 3-bromo monomer.

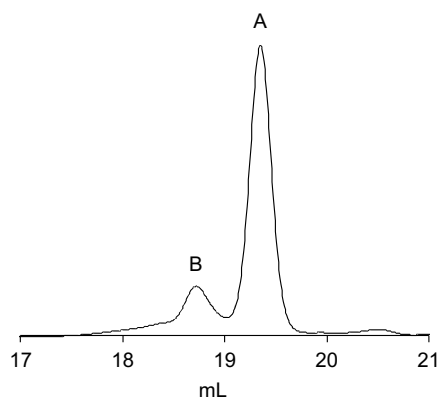


Figure S1. GPC profile of the product obtained after SiO₂ column chromatography in the cyclization of **4** using SiCl₄.

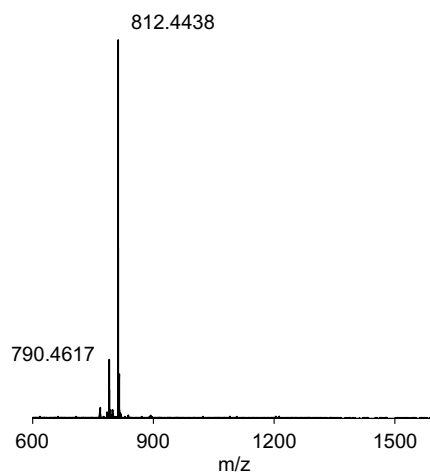


Figure S2. ESI-MS of isolated **DiMeO_C3A**.

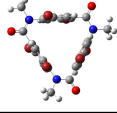
	Optimized structure	Energy/a.u.	$\Delta E/\text{kcal}\cdot\text{mol}^{-1}$
DiMeO_C3A-anti		-2003.6620	
DiMeO_C3A-syn		-2003.6734	-7.2
DiBr_C3A-anti		-16743.4225	
DiBr_C3A-syn		-16743.4316	-5.7

Figure S3. Optimized structure and energy of *anti*- and *syn*-stereoisomers of **DiMeO_C3A** and **DiBr_C3A**. The calculations were performed on Gaussian 09 (Revision E.01) package of programs using B3LYP/6-31G(d) level of theory. For saving the computational cost, the alkyl chain was replaced by the methyl group.

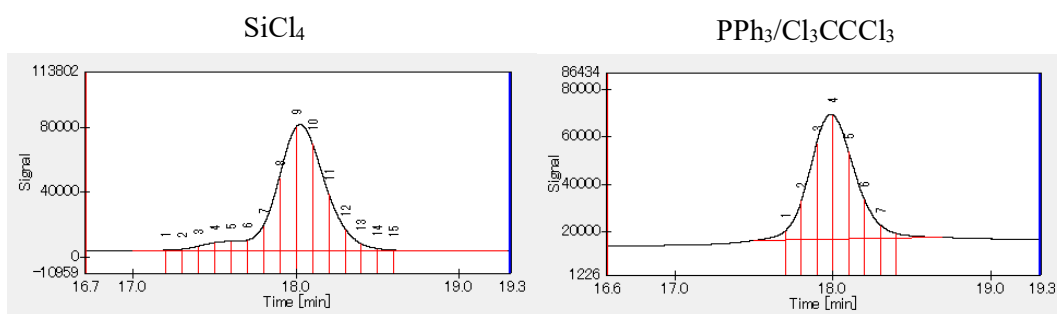


Figure S4. GPC profiles of the product obtained after SiO_2 column chromatography in the cyclization of **6** using SiCl_4 and $\text{PPh}_3/\text{Cl}_3\text{CCCl}_3$.

181016_infusion_22 #5-111 RT: 0.10-2.00 AV: 107 NL: 2.06E5
T: FTMS + p ESI Full ms [200.00-4000.00]

C45 H61 O3 N3 Br3: C45 H61 O3 N3 Br3 p(gss, sp:40) ...

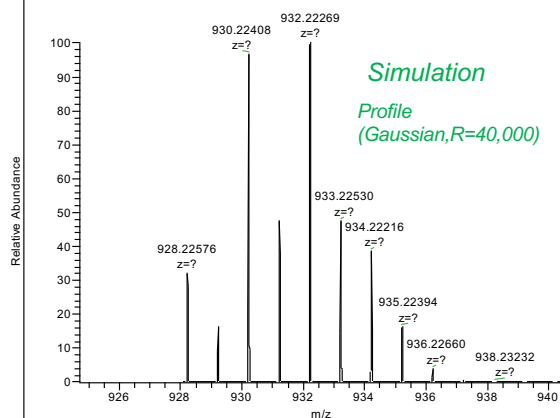
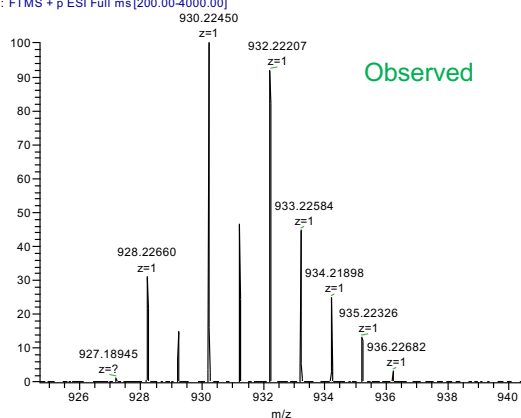


Figure S5. HR ESI-MS of **3Br_C3A** (left) and simulated pattern (right).

DQF-COSY

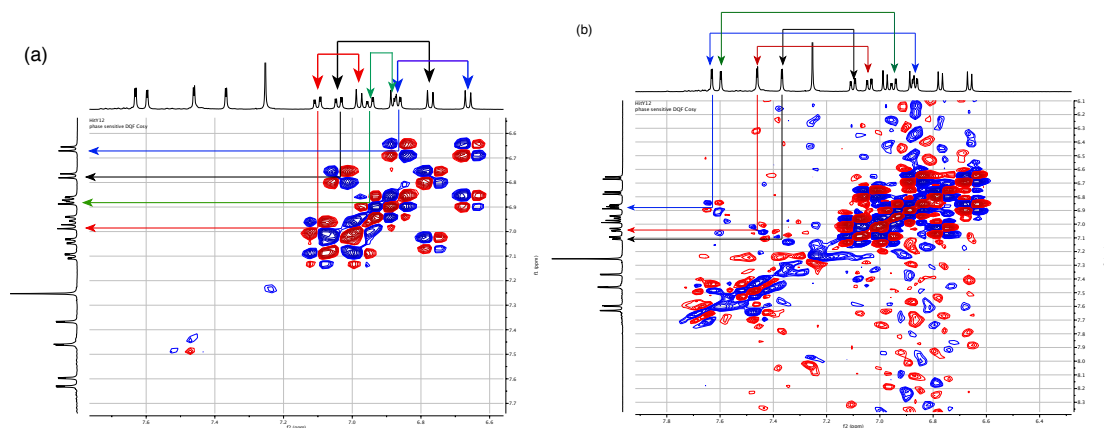


Figure S6. DQF-COSY charts of **3Br_C3A**.

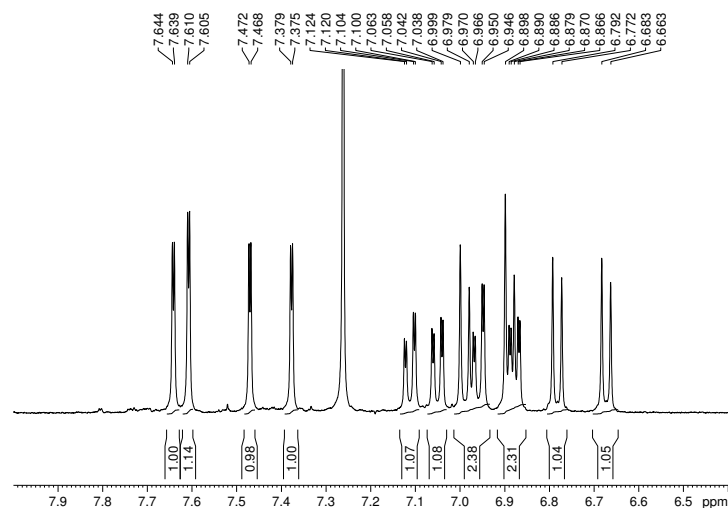


Figure S7. Expanded $^1\text{H-NMR}$ spectrum of **3Br_C3A** obtained at $100\text{ }^\circ\text{C}$ in CDCl_3 .

	Optimized structure	Energy/a.u.	$\Delta E/\text{kcal}\cdot\text{mol}^{-1}$
3Br_C3A-anti		-9030.0923	-1.1
3Br_C3A-syn		-9030.0906	
DiBr_C3A-anti		-16743.4225	
DiBr_C3A-syn		-16743.4316	-5.7

Figure S8. Optimized structure and energy of *anti*- and *syn*-stereoisomers of **3Br_C3A** and **DiBr_C3A**. The calculations were performed on Gaussian 09 (Revision E.01) package of programs using B3LYP/6-31G(d) level of theory. For saving the computational cost, the alkyl chain was replaced by the methyl group.

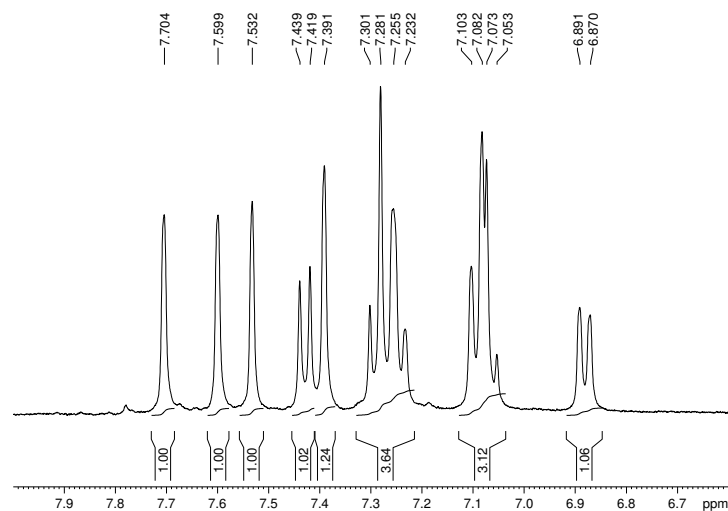


Figure S9. Expanded ^1H -NMR spectrum of **3Br_C3A** in DMSO-d_6 . Because of the insufficient solubility of compound, well-resolved coupling pattern of signals were lost.

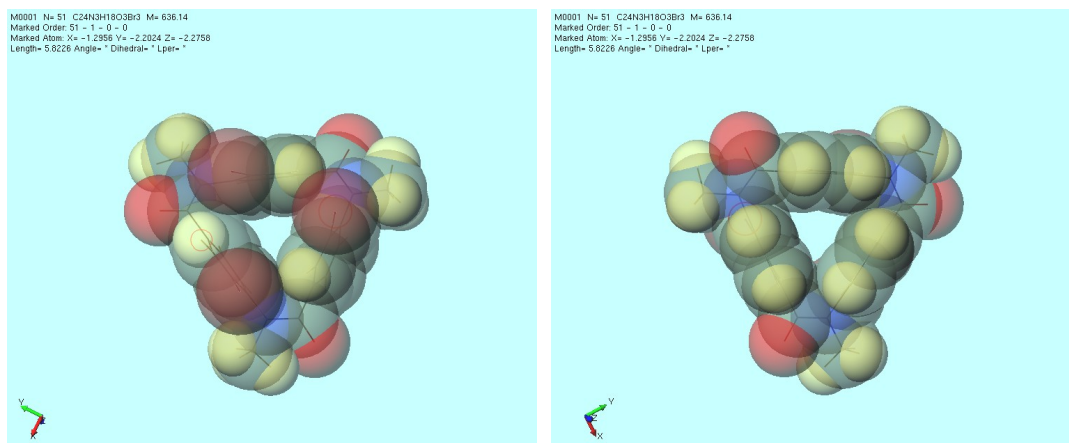


Figure S10. Space-filling model of the optimized structure of *syn*-stereoisomer of **3Br_C3A**. The octyl chains are replaced by the methyl groups for saving the computation cost.

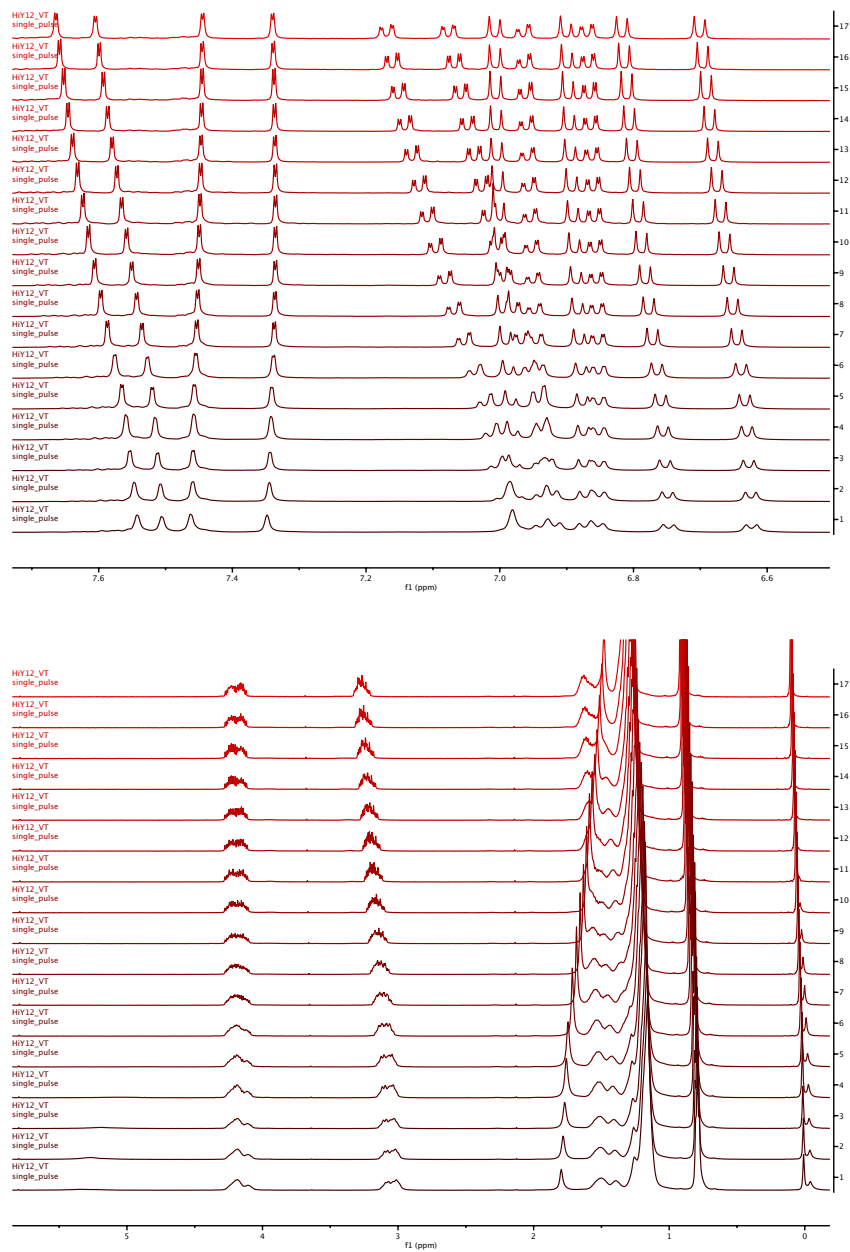


Figure S11. VT-NMR spectra of **3Br_C3A** at 100, 90, 80, 70, 60, 50, 40, 30, 20, 10, 0, -10, -20, -25, -30, -35, -40 °C (from top to bottom) on cooling. The spectra were recorded in 1,1,2,2-tetrachloroethane- d_2 .

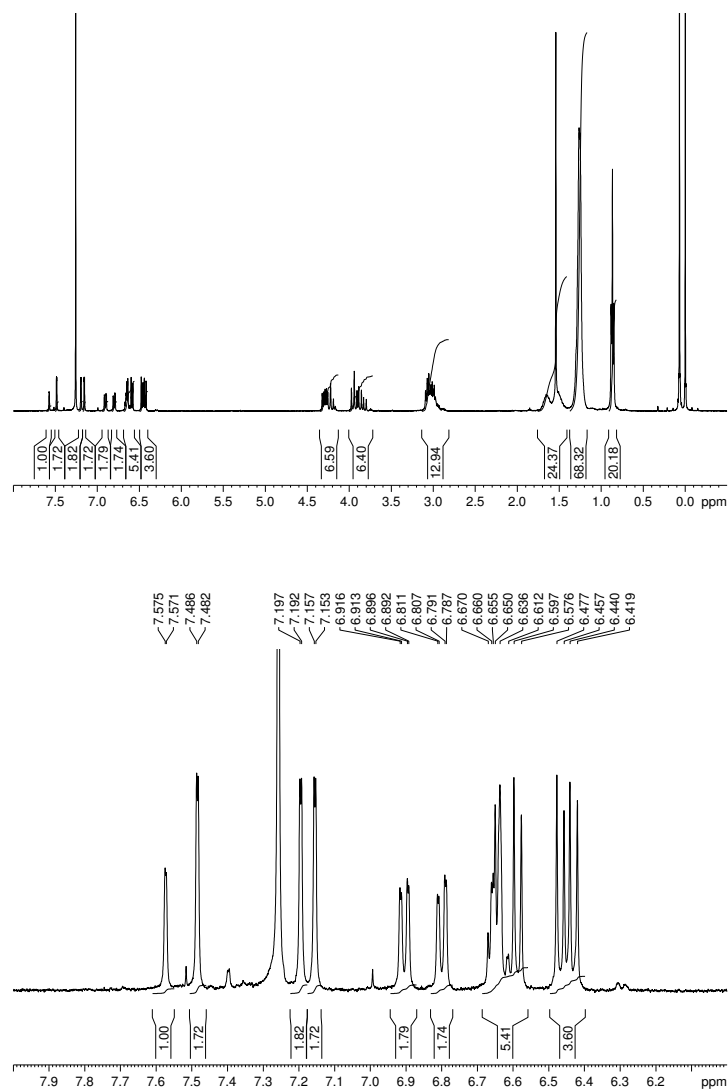


Figure S12. Full (top) and expanded (bottom) ¹H-NMR spectra of 3Br_C3Ared in CDCl₃.

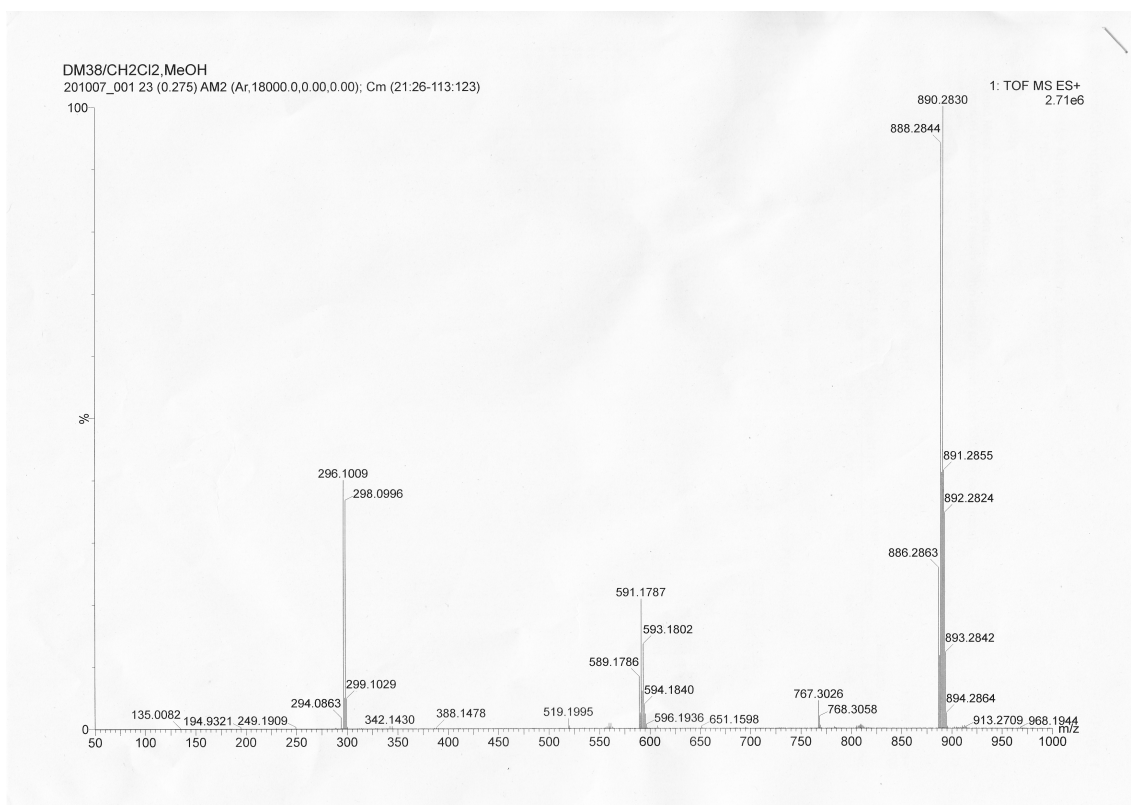


Figure S13. HR ESI-MS of **3Br_C3Ared**.